Preparation and Characterization of Dutasteride-loaded Nanostructured Lipid Carriers coated with Stearic Acid-Chitosan Oligomer for Topical Delivery

Norhayati Mohamed Noor[1,2], Khalid Sheikh[1], Satyanarayana Somavarapu[1], Kevin MG Taylor[1]

[1]Department of Pharmaceutics, UCL School of Pharmacy, 29-39 Brunswick Square, London WC1N 1AX, United Kingdom

[2]Institute of Bioproduct Development (N22), Universiti Teknologi Malaysia, 81310 UTM Johor Bahru, Johor, Malaysia

Corresponding authors: norhayati.noor.13@ucl.ac.uk, kevin.taylor@ucl.ac.uk,

ABSTRACT

Dutasteride, used for treating benign prostate hyperplasia (BPH), promotes hair growth. To enhance delivery to the hair follicles and reduce systemic effects, in this study dutasteride has been formulated for topical application, in a nanostructured lipid carrier (NLC) coated with chitosan oligomer-stearic acid (CSO-SA). CSO-SA has been successfully synthesized, as confirmed using ^{1}H NMR and FTIR. Formulation of dutasteride-loaded nanostructured lipid carriers (DST-NLCs) was optimised using a 2^3 full factorial design. This formulation was coated with different concentrations of stearic acid-chitosan solution. Coating DST-NLCs with 5% SA-CSO increased mean size from 187.6 ± 7.0 nm to 220.1 ± 11.9 nm, and modified surface charge, with zeta potentials being -18.3 ± 0.9 mV and $+25.8 \pm 1.1$ mV for uncoated and coated DST-NLCs respectively. Transmission electron microscopy showed all formulations comprised approximately spherical particles. DST-NLCs, coated and uncoated with CSO-SA, exhibited particle size stability over 60 days, when stored at 4-8°C. However, NLCs coated with CSO (without conjugation) showed aggregation when stored at 4-8°C after 30 days. The measured particle size for all formulations stored at 25°C suggested aggregation, which was greatest for DST-NLCs coated with 10% CSO-SA and 5% CSO. All nanoparticle formulations exhibited rapid release in an *in vitro* release study,

with uncoated NLCs exhibiting the fastest release rate. Using a Franz diffusion cell, no dutasteride permeated through pig ear skin after 48 h, such that it was not detected in the receptor chamber for all samples. The amount of dutasteride in the skin was significantly different ($p<0.05$) between DST-NLCs (6.09 ± 1.09 µg/cm^2) without coating and coated with 5% CSO-SA (2.82 ± 0.40 µg/cm^2), 10% CSO-SA (2.70 ± 0.35 µg/cm^2) and CSO (2.11 ± 0.64 µg/cm$^{2)}$. There was a significant difference ($p<0.05$) in the cytotoxicity (IC$_{50}$) between dutasteride alone and in the nanoparticles. DST-NLCs coated and uncoated with CSO-SA increased the maximum non-toxic concentration by 20-fold compared to dutasteride alone. These studies indicate that a stearic acid-chitosan conjugate was successfully prepared, and modified the surface charge of DST-NLCs from negative to positive. These stable, less cytotoxic, positively-charged dutasteride-loaded nanostructured lipid carriers, with stearic acid-chitosan oligomer conjugate, are appropriate for topical delivery and have potential for promotion of hair growth.

Keywords: alopecia, chitosan conjugation, dutasteride, nanostructured lipid carriers, topical delivery

1.0   INTRODUCTION

Androgenic alopecia (AGA, male-pattern baldness) affects almost 50% of men during their lives [1]. Androgen is one of the prerequisites for male-pattern baldness [2]. Normally, patients with androgenic alopecia have higher levels of dihydrotestosterone (DHT) and 5-α reductase enzyme activity on their balding scalp area than those with a non-balding scalp area [3]. In hair-loss patients, testosterone is converted to DHT which results in miniaturization of the hair follicle and hair shedding [4]. There are two types of enzymes that contribute to androgenic alopecia: type I 5α-reductase enzyme is present in the skin, including scalp, and type II is in the hair follicles and prostate [5]. Dutasteride (a type I and type II 5α-reductase inhibitor) is approved by the US Food and Drug Administration (FDA) for treating benign prostate hyperplasia (BPH), and has been studied for hair growth efficacy, with an oral dose of 0.5 mg daily [6]. Dutasteride taken orally will reduce DHT levels throughout the body. In order to reduce the systemic effects of lowered DHT levels, such as diminished sexual desire, increased depression

and ejaculation disorder [7,8], topical administration of dutasteride for treating AGA would be an appropriate drug-delivery strategy. Little research has been conducted using dutasteride for topical application. Ansari et al. [9] prepared nanoemulsions using different ratios of oleic acid and eucalyptus oil for delivery to the skin, in the size range of approximately 20-210 nm; no information on surface charge, entrapment efficiency or drug loading was provided. Madheswaran et al. [10] used monoolein to produce liquid crystalline nanoparticles of finasteride and dutasteride, surface-modified with chitosan (low molecular weight) to give a positive charge. The mean particle size was 239-259 nm, with zeta potential +19.8 to +48.5 mV. The surface-modified nanoparticles enhanced transdermal delivery of the 5-α reductase inhibitors, increasing permeation of finasteride and dutasteride. No stability studies were undertaken. Unlike most previous studies of dutasteride employing oral administration, this work aims to achieve local delivery of dutasteride, by formulation in a nanostructured lipid carrier (NLC) system for topical delivery to the skin/hair follicles. Previous studies have determined the transfollicular delivery of materials, including drugs using nanoparticles. Lademann et al. [11] found that dye-containing nanoparticles with a mean size of 320 nm penetrated deeper into the hair follicles, when massage was applied, than the dye similarly applied in non-nanoparticulate form. Blume-Peytavi et al., [12] compared the transfollicular and percutaneous delivery of a minoxidil foam. Minoxidil was detected in the blood faster when the hair follicle orifices were opened compared to the blocked hair follicle orifices, demonstrating more rapid drug delivery and transport via the follicular route. Patzelt et al., [13] reported that the penetration depth of particles into the hair follicles was dependent on their size; medium sized particles (643 and 646 nm) penetrated deepest into porcine hair follicles, whereas smaller (122 nm, 230 nm, 300 nm and 470 nm) and larger particles (860 nm, 920 nm and 100 nm), penetrated the follicle, but to shorter depths.

Nanostructured lipid carriers (NLCs) were introduced by Muller et al., [14] subsequent to solid lipid nanoparticles (SLNs), to overcome some of the limitations associated with SLNs. NLCs can increase loading capacity, physical and chemical long-term stability and prolong release of incorporated molecules. They are also suitable for topical formulations [15]. Different types of solid lipid can be used in the production of SLNs and NLCs. The term of solid lipid includes fatty acids (e.g. myristic, stearic and palmitic acid), triglyceride (e.g. tripalmitin and tristearin), diglyceride (e.g. glyceryl behenate),

monoglyceride (e.g. glyceryl monostearate), steroids (e.g. cholesterol) and waxes (e.g. cetyl palmitate and beeswax). Different types of solid lipid have different degrees of crystallization that may impact drug entrapment and loading, size and charge, and also efficacy. The lipid particle matrix is solid at both ambient and body temperatures [16]. In this study, stearic acid has been chosen as a solid lipid due to its potential for promoting hair growth [17]. Previous research [18] has demonstrated that free fatty acids (α-linolenic, linoleic, palmitic, elaidic, oleic and stearic acid) are potent 5α-reductase inhibitors and promote hair regrowth. Inclusion of stearic acid in the formulation, might have an additional effect with dutasteride for the promotion of hair growth. Due to the properties of dutasteride, which is poorly water soluble (0.038 ng/mL; Log P=5.09) [19], NLCs would seem useful as a potential carrier. NLCs composed of biocompatible and biodegradable lipids have low toxicity and cytotoxicity, are suitable for topical application and have an occlusive effect on the skin, increasing skin hydration [20]. Mittal et al. [21] reported that NLCs with a size of approximately 300 nm were found in the transfollicular region of the skin. Hamishehkar et al. [22] found higher skin deposition of flutamide-loaded SLNs (volume mean diameter approximately 200 nm) compared to flutamide hydroalcoholic. This higher accumulation of flutamide-SLNs in the hair follicles suggested a greater growth of new hair follicles based on the histological assessment

Chitosan, a naturally occurring polysaccharide, contains free amino groups, is cationic in neutral or basic pH conditions, and is commonly used for drug delivery applications, particularly where a positive charge is advantageous. Hair is negatively charged [23]; consequently, introducing a positive charge to nanoparticles may enhance targeting. It is also reported that due to the bioadhesive properties of chitosan, it may increase retention of the drug/carrier in the targeted area [24]. Taking this into account, DST-NLCs coated with a positively-charged, chitosan-based polymer have been investigated here for topical/transfollicular delivery.

In the present study, stearic acid was selected for use as a lipophilic ingredient and synthesized with chitosan to enhance the lipophilicity of the aqueous-soluble chitosan. The carboxylic group of stearic acid was reacted with the amine group from chitosan with addition of 1-ethyl-3-(3-dimethylaminopropyl) carbodiimide hydrochloride (EDC.HCl), creating the hydrophobic drug-delivery moiety.

Therefore, it is suggested that when dutasteride is incorporated in the nanostructured lipid carrier (NLC), the drug will be entrapped in the hydrophobic region where surfactants are added to stabilize it. A solution of stearic acid-chitosan (CSO-SA) having a positive charge will coat the nanoparticles.

The aim of this study is then to design and formulate a stable and less cytotoxic formulation of DST-NLCs coated with CSO-SA for the promotion of hair growth. This study anticipates that surface modification of DST-NLCs with CSO-SA would produce a slow release of the drugs in the skin/hair follicles with potential to reduce systemic effects.

2.0   MATERIALS AND METHODS

2.1   Materials

Stearic acid was purchased from Tokyo Chemical Industry (UK). Chitosan oligomer (CSO), Mwt <3000Da and dutasteride (purity >98.0%) were obtained from Carbosynth (UK). Ethanol (96% v/v analytical grade), 1-ethyl-3-(3-dimethylaminopropyl) carbodiimide hydrochloride (EDC.HCl), ninhydrin, Sephadex G-50 and acetic acid-d_4 (99.9 atom %D) were obtained from Sigma-Aldrich (UK). Deuterium oxide (99.9 atom %D) was purchased from Cambridge Isotope Lab. Inc. (USA), Phosal® 53 MCT and Lutrol® micro 68 were supplied by Lipoid GmbH (Germany) and BASF Group (Ludwigshafen, Germany), respectively. Acetone, water (HPLC grade) and acetic acid glacial (analytical reagent) were purchased from Fisher Scientific (United Kingdom). Deionized water was prepared in-house (PURELAB, ELGA, UK).

2.2   Synthesis of stearic acid-chitosan (CSO-SA)

Chitosan oligomer (CSO) was conjugated by the reaction of the carboxyl groups of stearic acid in the presence of EDC.HCl with the free amino groups of chitosan oligomer

(Fig.1), using an established method with minor modifications [25,26]. CSO (1 g) was dissolved in 120 mL of deionized water with magnetic stirring for 2 h at 80°C. Meanwhile, 0.5 g stearic acid (SA) was dissolved in ethanol (80 mL) and heated at 60°C, with stirring. SA solutions were activated by EDC.HCl (1:5 molar ratio) and stirred for 2 h at 60°C. The solutions of SA were then added using a syringe with needle (BD Micro Lance™ 3, Spain) into the CSO solution with continuous stirring for 6 h.

The product was evaporated under vacuum (Buchi Rotary evaporator, Buchi, Switzerland) at 70°C to reduce the volume. Unreacted EDC.HCl and SA were removed by dialysis (Mwt cut-off 1000 Da, Spectrum Laboratories, USA) for 2 days, then the product precipitated using 300 mL of acetone and filtered using filter paper (Fisherbrand QL100, Fisher Scientific, UK). This precipitation/filtration step was repeated three times. Samples were stored in a desiccator for further analysis.

2.2.1 Characterization of chitosan oligomer-stearic acid using Fourier Transform Infrared Spectroscopy (FTIR)

Samples of CSO-SA, CSO and SA were analysed using FTIR to confirm the presence of the SA group in the CSO chain. Samples were analysed with 4 scans from 660 to 4000 cm^{-1} using PerkinElmer Spectrum100 FTIR (PerkinElmer, UK). The spectrum of CSO-SA was then compared to those of pure CSO and SA.

2.2.2 Characterization of chitosan oligomer-stearic acid using ^{1}H NMR

In order to confirm the presence of the fatty acid chain in the chitosan conjugate, samples were characterised using nuclear magnetic resonance spectroscopy (NMR). 5 mg of CSO, CSO-SA and SA was dissolved in 1 mL of deuterium oxide (D_2O) with the addition of one drop of acetic acid-d_4 in order to dissolve the product. The ^{1}H NMR spectra were obtained using a NMR Bruker Avance 500 spectrometer (Bruker Instruments, USA).

2.2.3 Determination of amine group substitution using ninhydrin assay

The amount of chitosan conjugated with stearic acid was determined using ninhydrin as a reagent to react with the primary and secondary amino groups in the conjugated product [27]. The percent of free amino groups present in the CSO-SA conjugate was determined using the ninhydrin assay, by assuming the D-glucosamine slope has 100% amine groups, and the CSO and CSO-SA were then identified by comparing each slope. Serial dilutions of D-glucosamine (stock solution: 500 µg/mL), CSO and CSO-SA (stock solution: 2000 µg/mL) were prepared in 0.2% acetic acid solution. The working solutions for CSO and CSO-SA were 100, 60, 40 and 20 µg/mL and for D-glucosamine 25, 20, 15, 10, 5 µg/mL. To prepare the ninhydrin solution, 0.35 g of ninhydrin was dissolved in 100 mL of ethanol.

To start the reaction, 0.5 mL of CSO or CSO-SA solutions, 0.5 mL of 4M acetate buffer (pH 5.5) and 2 mL of ninhydrin solution were combined and heated at 90°C in a water bath with stirring for 15 min, then cooled to room temperature. The solution was then made up to 10 mL with ethanol. The absorbance was measured at 570 nm using Agilent Cary 100 UV-Vis Spectroscopy (Agilent Technologies UK Ltd., Berkshire, UK). The amounts of free amine groups in CSO and CSO-SA samples were assigned by comparing the slopes using linear regression from D-glucosamine where the absorbance (y) for each sample was plotted as a function of concentration (x).

2.3 Preparation of dutasteride-loaded nanostructured lipid carriers (DST-NLCs)

DST-NLCs were prepared by the melt-dispersion ultrasonication method [28–30]. Dutasteride (5 mg), stearic acid and Phosal® 53 MCT were weighed into a glass vial. Lutrol® micro 68 was added into another glass vial with water (10 mL). Both glass vials were heated separately at 80-90°C in a water bath. When the drug completely dissolved in the liquid lipid (by magnetic stirring), the aqueous solution was added into the oil-phase solution. The mixture was homogenized using an IKA Ultra Turrax T25 (IKA Werke, Germany) at 19,000 rpm for 10 min. The hot solution was further processed using a probe-type sonicator (MSE Soniprep 150, MSE, UK) at 18W, for 5 min. 2 mL

of hot dispersion was syringed (needle: 25 gauge, 5/8th inch) into 10 mL of cold water (4-8°C) and stirred for 10 min to obtain nanoparticles. The formulation was stored at 4-8°C before being characterised. The weight of dutasteride was 5 mg, and 10 mL of water was used for all formulations.

2.3.1 Experimental design of preparation of DST-NLCs using 2^3 full factorial design

The amount of solid lipid and surfactant used to prepare DST-NLCs was varied to obtain the smallest mean particle size, narrowest size distribution, and highest entrapment efficiency and drug loading. This was achieved with a 2^3 full factorial design, Design Expert 6.0.8 Software (Stat-Ease, USA). The three factors evaluated were: the content of stearic acid (*A*), Lutrol® micro 68 (*B*) and Phosal® 53 MCT (*C*) (Table 1).

A factorial design was used to obtain maximum information, such as the interaction between the factors, whilst minimising the number of experiments [31]. The design required, in total, 8 preparations. The experiments were repeated three times to calculate the experimental error.

2.3.2 Preparation of DST-NLCs coated with chitosan oligomer (CSO) and stearic acid-chitosan (CSO-SA)

The optimised DST-NLC preparation was chosen based on statistical analysis. The formulation was scaled up from 100 mg to 300 mg of stearic acid to allow use of the desired concentration of dutasteride (approximately 0.3 mg/mL). Quantities of other materials (dutasteride, Phosal® 53 MCT and Lutrol® micro 68) were up-scaled using the same ratio, with water kept constant at 10 mL. The amount of dutasteride was optimised between 15 and 20 mg. CSO-SA (5 or 10 % of solid lipid content) and CSO (5% of solid lipid content) were dissolved in acidified water (0.2% acetic acid in deionized water). 250 µL of the solution was added, using a syringe (needle: 25 gauge, 5/8th inch), into 5 mL of DST-NLCs with constant stirring for 10 min.

2.4   Characterization of DST-NLCs, uncoated and coated with CSO-SA or CSO

2.4.1   Measurement of particle size distribution, zeta potential and determination of nanoparticle morphology

The size distribution and zeta potential of nanoparticles were obtained as Z_{Ave} hydrodynamic diameter, polydispersity index (PDI) and zeta potential (ξ) using a Zetasizer Nano ZS (Malvern Instruments, UK) after 1 day, at 25°C. Formulations were prepared with deionized water (pH 5.6) and used without further dilution. 1 mL of the sample was pipetted directly into the zeta potential DTS1070 folded capillary cell (Malvern, UK) without dilution. Measurements were performed 3 times, and mean values were taken. Zeta potential was calculated from electrophoretic mobility using the Helmholtz-Smoluchowski equation by the Malvern data analysis software..

The morphology of the nanoparticles was determined using transmission electron microscopy (TEM; Philips/FEI CM120 Bio Twin, FEI Netherlands). Samples were placed on copper grids for viewing and excess droplets were wicked away with filter paper [32]. After 2 min, a drop of 1% phosphotungstic acid was placed onto the copper grid for negative staining. The grid was dried at room temperature and observed using TEM.

2.4.2   Entrapment efficiency and drug loading

Entrapment efficiency and drug loading were calculated as described previously [33], with modification. Entrapment efficiency and drug loading were determined using Sephadex® gel G-50 as a mini column. 5 mL of gel was packed in a 5 mL syringe, placed in a centrifuge tube (size of 50 mL) and centrifuged at 1000 rpm (angle rotor 19776-H, at 104 x *g*) for 10 s in a refrigerated centrifuge (Sigma Laborzentrifugen, Germany) at 20°C to remove excess water. Then, 0.5 mL DST-NLC preparation was pipetted in the middle of the column and separated by column chromatography at 1000 rpm for 5 min. The column was washed with 0.5 mL deionized water at 1000 rpm for a further 5 min. The collected sample, dutasteride entrapped in NLCs, was diluted with ethanol in a 10 mL volumetric flask and sonicated for 10 min to dissolve the particles

before filtration using a 0.22 µm pore size syringe filter (Merck Millipore, Ireland). Unentrapped dutasteride was retained in the Sephadex G-50 gel. The ethanolic solution was assayed using a validated HPLC method to determine the total and entrapped dutasteride in the DST-NLCs.

High performance liquid chromatography (HPLC) with UV/Vis detector (Agilent 1100 Series, USA) at wavelength 241 nm was used to quantify dutasteride in preparations. The analytical column, Synergi™ 4 µm Polar-RP 80 Å, 250 x 4.6 mm was selected as the stationary phase. Separation was carried out using a mobile phase 70:30 (by volume) of acetonitrile and 0.1% trifluroacetic acid (TFA) in HPLC grade water. The injection volume used was 30 µL at 1 mL/min flowrate.

Encapsulation efficiency was calculated from the amount of entrapped (n_1) and total dutasteride in the preparation (n_2) (Equation 1). Dutasteride loading was calculated using Equation 2.

$$\textbf{Entrapment efficiency (\%)} = \frac{\boldsymbol{n_1}}{\boldsymbol{n_2}} \times \textbf{100} \qquad\qquad \textbf{Equation 1}$$

where;

n_1 = concentration of entrapped dutasteride in DST-NLCs

n_2 = total concentration of dutasteride in DST-NLCs

$$\textbf{Drug loading (\%)} = \frac{\boldsymbol{C_1}}{\boldsymbol{C_0}} \times \textbf{100} \qquad\qquad \textbf{Equation 2}$$

where;

C_1 = total weight of entrapped dutasteride in DST-NLCs

C_0 = total weight of solid lipid, surfactant and dutasteride in DST-NLCs

2.4.3   Stability study

The stability of DST-NLCs was investigated to explore potential changes in the size distribution and surface charge with time. Each formulation was stored in a refrigerator

10

at 4-8°C and at 25°C (incubator). Particle size distribution and zeta potential were compared at day 1, 30 and 60.

2.5 *In vitro* drug release

In vitro release was studied using a Franz diffusion cell (PermeGear, USA). A 0.45 µm HA nitrocellulose membrane (MF™ Membrane Filters, Merck Millipore, Ireland) was mounted in the Franz diffusion cell (surface area = 0.64 cm^2) maintained at 37°C and stirred using a magnetic stirrer (600 rpm). Due to the limited solubility of dutasteride in phosphate-buffered saline (PBS), 2% sodium dodecyl sulphate (SDS) was added. DST-NLCs, with or without chitosan (250 µL), were pipetted in the donor chamber and sampling (200 µL) was done at 0, 0.25, 0.5, 1, 2, 3, 6, 8, 12, 24, 30 and 36 h from the receptor chamber, replaced with 200 µL fresh buffer. Samples were injected into the HPLC to determine drug released.

2.6 *In vitro* permeation

An *in vitro* permeation study was conducted to quantify the amount of drug present in the skin and potential systemic exposure. In order to mimic topical application of the formulation, *in vitro* permeation was performed using a vertical Franz diffusion cell (PermeGear, USA). Pig ears were obtained from a local slaughterhouse (Farnborough, UK) from a freshly slaughtered pig (used for food consumption). The ears were washed with deionized water and hairs were trimmed carefully with scissors. The pig ear skin was excised using a scalpel and forceps and the subcutaneous tissue was removed. The average thickness of the skin was ~0.5 mm. The skin was cut and frozen (-20°C) for future use.

The diffusion surface area of the Franz cell was 0.64 cm^2. The receptor chamber was filled with 5 mL of PBS (pH 7.4) with 2% SDS and 0.02% sodium azide and maintained at 37°C whilst being stirred using a magnetic stirrer. The skin was mounted between the donor and receptor chambers and allowed to equilibrate for 1 h. 250 µL of DST-NLCs formulation, with or without chitosan, was pipetted in the donor chamber.

200 µL samples were withdrawn at 0, 0.25, 0.5, 1, 2, 3, 6, 8, 12, 24, 30, 36 and 48 h, and 200 µL fresh buffer added to the receptor chamber. Nanoparticle formulations were compared to ethanolic solutions of dutasteride (0.29 mg/mL in 70% ethanol). After 48 h, the stratum corneum was removed using a tape stripping method. The epidermis/dermis was chopped into small pieces using a scalpel and stirred for 24 h with ethanol and sonicated for 1 h. The solution was filtered and injected into the HPLC for quantification of the drug which permeated in the skin.

2.7 *In vitro* cytotoxicity study on hair follicle dermal papilla cells

In order to determine the maximum non-toxic concentration (EC90) of unencapsulated and encapsulated dutasteride in nanoparticles, MTT assays on normal hair follicle dermal papilla cells were undertaken. Human hair follicle dermal papilla cells (HFDPCs) (Promo- Cell, Germany) were grown in HFDPCs growth medium (Promo-Cell, Germany) containing 100 IU/ml penicillin/streptomycin (Gibco-BRL, USA) and 2.5 µg/ml of amphotericin B (Sigma-Aldrich, UK) in a humidified 95% atmosphere with 5% CO_2 at 37°C. Cultured HFDPCs from passage 4 were seeded (3.75 x 10^4 per mL) into 96-well plate (Nunc, Wiesbaden, Germany) and grown to a confluence of 60–70% for 24 h. The MTT assay was conducted for 5 days with dutasteride alone (dutasteride alone was dissolved in DMSO at 100 mM and serial dilutions were prepared from 100 to 1.6 µM), dutasteride in the nanoparticles coated or uncoated with CSO-SA (12.5 - 100 µM) and empty NLCs coated and uncoated with CSO-SA (at the same concentration as DST-NLCs and DST-NLCs CSO-SA). MTT (5 mg/mL) was added to each well, and cells were incubated for 4 h at 37°C. The supernatant was then removed, and 100 µL of dimethylsulfoxide was added to dissolve formazan products. Absorbance was determined spectrophotometrically at 570 nm using microplate reader (SpectraMax®M2e, Molecular Devices, USA). Results were expressed as percentages of untreated controls in four cultures. Reported values represent means ± SEM.

2.8   Statistical analysis

All data were analysed either using a t-test or one-way ANOVA and Tukey's post-hoc test, using IBM SPSS Statistic 22, except data from the experimental design for the model (formulations) which were analysed using Design Expert 6.0.8 Software (Stat-Ease, USA). A p-value of less than 0.05 was considered significant.

3.0   RESULTS AND DISCUSSION

3.1   Synthesis and characterization of CSO-SA

3.1.1 ^{1}H NMR and FTIR

Formation of the CSO-SA conjugate was determined using FTIR and ^{1}H NMR. The IR spectrum of CSO-SA showed two peaks at around 1636 and 1584 cm^{-1} corresponding to the N-stearoyl (amide bond) (Fig. 2a). The increase of the C-H absorption around ~2855 cm^{-1} indicated the presence of the stearoyl chain. The chemical shifts shown at 1.0 - 1.1 ppm in the NMR spectrum represent protons from CH$_3$ of stearic acid whereas the peaks at 1.13 - 1.15 ppm correspond to protons of CH$_2$ in the acyl chain (Fig. 2b). This finding agrees with previous studies [34,35]. The remaining peaks are due to hydrogen from the chitosan oligomer, indicating that stearic acid was conjugated to the chitosan oligomer.

3.1.2   Degree of substitution determined by ninhydrin assay

Based on the ninhydrin assay, the slopes for D-glucosamine and chitosan oligomer (CSO) and CSO-SA were 0.0676, 0.0126 and 0.0093, respectively. The number of amine groups on the chitosan oligomer was found to decrease due to the substitution of stearic acid. By comparing the slope from D-glucosamine and CSO; the percent degree of substitution (%DS) of CSO-SA was calculated to be 6.0%.

13

3.2 Preparation, optimization and characterization of DST-NLCs coated and uncoated with CSO-SA/CSO

3.2.1 Factorial design results on particle size distribution of DST-NLCs

DST-NLCs were prepared according to a design of experiments. The main independent factors that might influence the particle size distribution were the contents of stearic acid, Lutrol ® F68 and Phosal® 53 MCT. All of the formulations gave mean size larger than 100 nm (Fig. 3).

Experimental design was employed to find the best model that relates the ratio of solid lipid and surfactant to mean particle size and PDI (a measure of the width of the size distribution). At day 1, there was no significance model term for the hydrodynamic diameter results ($p>0.05$), suggesting high stability of the particles for the quantities of materials used. To obtain optimised, stable particles, the NLCs were stored at 4-8°C for 14 days (Fig. 3), revealing a significant difference in the model term for the hydrodynamic diameter at day 14 ($p<0.05$).

From the modelling at day 14, the 'Predicted R-Squared' (0.8058) was in reasonable agreement with the 'Adjustment R-Squared' (0.9150). Table 2 shows the results of ANOVA on hydrodynamic diameter at day 14, indicating that some formulations were unstable, with increased hydrodynamic diameters after two weeks. The mathematical modelling of DST-NLCs on hydrodynamic diameter followed Equation 3 (coded value at day 14):

Hydrodynamic diameter (nm) = 344.60 – 73.35*A

$$+ 31.10*B - 78.90*A*B \qquad \textbf{Equation 3}$$

Where;

A – Stearic acid

B – Lutrol® micro 68

C – Phosal® 53 MCT

Fig. 4a shows the interaction between stearic acid (*A*) and Lutrol® micro 68 (*B*) on hydrodynamic diameter. 100 mg stearic acid, 50 mg Lutrol® micro 68 and 25 or 50 mg Phosal® 53 MCT produced the smallest particles (S4 and S8), having a mean diameter of 223.5 nm. Increasing surfactant content stabilized the nanoparticles, with a reduction in mean size. Hydrophilic-Lipophilic Balance (HLB) is a major consideration in making stable emulsions. In this study, Lutrol ® F68 has a high HLB value (>24) and soy phosphatidycholine (53% in Phosal® 53 MCT) has a low HLB value (4). Using a mix of emulsifiers can stabilize the emulsion in terms of coalescence rate [36].

Model *A*, *C*, *AB* and *AC* were significantly different ($p<0.05$) on PDI at day 14 (Table 3). 'Predicted R-Squared' (0.9761) from the model was in reasonable agreement with the 'Adjustment R-Squared' (0.9948).   Equation 4 shows the model for PDI at day 14 (in coded value).

(PDI) = 0.23 – 0.048*A + 4.750 x 10^{-3}*B + 0.042*C

– 0.038*A*B – 0.015*A*C **Equation 4**

where;

      A – Stearic acid

      B – Lutrol® micro 68

      C – Phosal® 53 MCT

Figs. 4b and 4c show a 3D-surface graph of the interaction between stearic acid (A), Lutrol® micro F68 (B) and stearic acid with Phosal® 53 MCT (*C*). 100 mg stearic acid, 50 mg Lutrol® micro 68 and 25 mg Phosal® 53 MCT (Formulation S4), produced NLCs with a narrow particle size distribution (PDI=0.123). When the amount of surfactant was increased, PDI decreased with a mondispersed size distribution. It has been shown in the previous research that by increasing the surfactant, the particle size was decreased at certain concentration [36]. At low concentrations of surfactant, aggregation is accelerated where the fraction of particle surface area which is coated remains small. At higher surfactant concentration, all the agglomerated particles are coated and the particle size is reduced [36]. This allows ease of dispersion, reduced aggregation and hence a reduction in PDI.

3.2.2 Factorial design results for surface charge

Fig. 5 shows all particles had negative charge due to the presence of the stearic acid. There was no significant difference (ANOVA, $p>0.05$) on the model for zeta potential at day 1 or day 14. Based on the results for hydrodynamic diameter and PDI, formulation S4 and S8 were chosen and further analysed using a t-test, which revealed no significant difference ($p>0.05$) for zeta potential between S4 and S8.

3.2.3 Factorial design results for entrapment efficiency and drug loading

The entrapment efficiency (%EE) for all formulations was greater than 60% (Table 4). Table 5 shows ANOVA results for entrapment efficiency. Based on the results (Fig. 6), model *A* and *AB* were significantly different ($p<0.05$). Based on the model, 100 mg stearic acid, 50 mg Lutrol® micro 68 and 25 or 50 mg Phosal® 53 MCT produced highest entrapment efficiency (95.1%). The content of stearic acid and the interaction between stearic acid and Lutrol® micro 68 significantly impacted EE% ($p<0.05$). However, there was no significant impact on drug loading ($p>0.05$), with the mean drug loading for all formulations being in the range 2 to 4.40%.

The mathematical modelling of entrapment efficiency for DST-NLCs followed Equation 5 (coded value):

$$\textbf{EE\% = 82.14 + 10.24*A} - \textbf{2.61*B + 5.29*A*B} \qquad \textbf{Equation 5}$$

Where;

       A – stearic acid

       B – Lutrol® micro 68

       C – Phosal® 53 MCT

3.2.4 Stability of DST-NLCs on storage

Hydrodynamic diameter and particle size distribution were studied on day 1 and 14 (Fig. 3). There were no significant differences ($p>0.05$) in the hydrodynamic diameter at day 1. At day 14, some formulations demonstrated an increase in mean size,

especially S3 and S7. This may be due to the amount of surfactant present being insufficient to stabilize the formulations. The results indicate that the ratio of contents in S4 (100 mg stearic acid, 50 mg Lutrol® micro 68 and 25 mg Phosal® 53 MCT) and S8 (100 mg stearic acid, 50 mg Lutrol® micro 68 and 50 mg Phosal® 53 MCT) gave the smallest hydrodynamic diameter and PDI at day 1 and day 14. There was no significant difference ($p>0.05$) between S4 and S8 at day 1, and 14 with respect to hydrodynamic diameter and PDI. Consequently, Formulation S4 was selected for the subsequent investigations.

3.2.5 Effect of scale-up of the DST-NLCs preparation

Formulation S4 was selected, as indicated above, and production quantities scaled up 3x. Mean hydrodynamic diameter and PDI were not significantly altered ($p>0.05$; data not shown). Then, the amount of dutasteride was varied and 17.5 mg dutasteride was found to be the optimal content, giving highest entrapment efficiency ($97.8 \pm 0.68\%$). When drug content was increased to 20 mg, entrapment efficiency decreased to $90.1 \pm 1.07\%$, indicating the limitation of the amount of drug that can be loaded in this carrier system, as reported previously [37]. Furthermore, there was no significant difference ($p>0.05$) in drug loading ($3.49 \pm 0.10\%$).

3.2.6 Particle size distribution of DST-NLCs uncoated and coated with CSO-SA and CSO

The nanoparticles were coated with CSO and CSO-SA using a physical adsorption method. There was a significant increase in mean size following coating ($p<0.05$), from 187.6 ± 7.0 nm to 220.1 ± 11.9 nm and 230.1 ± 8.2 nm when coated with 5 and 10% CSO-SA, respectively. Coating with 5% CSO, the size was 208.4 ± 1.6 nm ($p>0.05$). There was not significant difference ($p>0.05$) in PDI for the preparations, with mean PDI <0.2, indicating all had narrow size distributions.

Based on the TEM images, uncoated DST-NLCs and those coated with CSO/CSO-SA were spherical (Fig. 7) and in the size range approximately 200-250 nm. There was some

suggestion of aggregation for DST-NLCs coated with 10% CSO-SA (Fig. 7D), probably due to the higher concentration of CSO-SA.

3.2.7 Zeta potential of DST-NLCs before and after coating

The zeta potential of DST-NLCs changed from negative to positive on coating ($p<0.05$), with CSO-SA or CSO adsorbed to negatively-charged DST-NLCs, producing positively-charged nanoparticles. Zeta potential value was increased from +26.0 ± 1.1 mV to +30.0 ± 1.2 mV for 5% to 10% of CSO-SA ($p<0.05$). The charge was higher for DST-NLCs coated with 5% CSO-SA than with 5% CSO (21.7 ± 2.1mV) ($p<0.05$). These findings indicated good interaction between DST-NLCs and CSO-SA, stabilizing the nanoparticles. This may result in part, from CSO-SA having some amphiphilic properties, as reported by Hu et al. [35] who produced stable doxorubicin-loaded polymeric micelles of a chitosan oligosaccharide-stearic acid conjugate. Moreover, the highly positively-charged CSO-SA will be electrostatically attracted to the negatively-charged surface of DST-NLCs. Previous studies [24,38–41] have demonstrated the electrostatic interaction between positively-charged chitosan and negatively-charged nanoparticles.

3.2.8 Stability of DST-NLCs uncoated, and coated with CSO-SA and CSO

DST-NLCs coated with 10% CSO-SA and 5% CSO aggregated when stored at 25°C (Table 6). However, uncoated DST-NLCs and those coated with 5% CSO-SA and 10% CSO-SA were stable at 4-8°C over a period of 60 days. DST-NLCs coated with 5% CSO-SA and 10% CSO-SA, had unchanged mean particle size and PDI at day 1, 30 and 60 ($p<0.05$). However, DST-NLCs coated with 5% CSO demonstrated physical instability, with aggregation even when stored at 4-8°C (day 30), possibly due to differences in the physical properties of the CSO compared to CSO-SA.

When uncoated DST-NLCs and those coated with 5% CSO-SA were stored at 25°C, the mean particle size increased by 2-fold compared to samples stored at 4-8°C. NLCs coated with 5% CSO, stored at 25° were aggregated at day 30. This might be due to the changes in polymer behaviour at different temperatures [42]. Increasing the

concentration of CSO-SA from 5% to 10% produced aggregation, possibly resulting from excess CSO-SA in the formulation, not associated with the NLC coating. The data indicate NLCs coated with chitosan without conjugation were relatively unstable. Having the hydrophobic chain (steroyl chain) in the chitosan-conjugate may enhance the stability of the nanoparticles, when the CSO-SA (at an appropriate concentration) was employed as a coating material.

3.2.9 *In vitro release* from uncoated and coated DST-NLCs

All nanoparticle preparations showed rapid release over the first 12 h (Fig. 8), with uncoated DST-NLCs exhibiting fastest release ($p<0.05$). There was no significant difference ($p>0.05$) between DST-NLCs coated with 5% and 10% CSO-SA, both having approximately 60% drug release at 36 h.

DST-NLCs without coating showed 72% release at 24 h. DST-NLCs coated with CSO-SA had a lower drug release due to the presence of the polymer in the outer regions of the particles. In contrast, DST-NLCs coated with 5% CSO (no conjugation) showed a slower release where $40.7 \pm 5.1\%$ of drug has been released at 36 h. Dutasteride in 70% ethanol (as control) showed only $32.6 \pm 10.7\%$ release at 36 h into the receptor media, probably due to the limited solubility of dutasteride in the receptor media. No precipitation was observed in the donor chamber after the experiment. The result was similar to that described previously whereby diphencyprone (slightly soluble in water) was released more slowly from ethanolic solution than from NLCs or a nanoemulsion formulation [43].

3.2.10 *In vitro* permeation

In vitro permeation studies using pig ear skin were conducted to mimic human skin. The follicular structure of pig ear skin is very similar to humans where their infundibula extend deep in the dermis, as in humans [44]. For all formulations, no dutasteride was detectable by HPLC in the receptor chamber (LOQ = 3 µg/mL). Considering, the

amount of dutasteride present in the skin (Fig. 9), the highest permeation in the skin (12.62 ± 1.72 µg/cm^2) was found from the ethanol solution.

This result was in agreement with previous research, in that ethanol acts as a penetration enhancer in topical products [45]. There was a significant difference ($p<0.05$) in the amount of dutasteride in the skin from ethanol and the hydrophobic drug-nanoparticle formulation. There were significant differences in the amount of dutasteride in the skin ($p<0.05$) when DST-NLCs (6.09 ± 1.09 µg/cm^2) were coated with 5% CSO-SA (2.82 ± 0.40 µg/cm^2), 10% CSO-SA (2.70 ± 0.35 µg/cm^2) or CSO (2.11 ± 0.64µg/cm^2). This result was similar to previous research [46] where they found benzophenone-3 loaded chitosan coated polymeric nanocapsules was less in the dermis and epidermis compared to uncoated with chitosan. These results could be discussed by the different surface charge between polysaccharide from chitosan and the epithelium as previously discussed for the ocular epithelium [47] and also the bioadhesive characteristic of chitosan [48]. Further experiments such as *in vivo* studies are required to confirm these formulation effects on permeation. In normal application, the same concentration of dutasteride will be applied on the scalp where the surface area will be much higher. Moreover, massaging of the scalp which will increase the total amount of the drug in the skin, since previous research has shown such massage resulted in deeper penetration of nanoparticles in the hair follicular region[11]. The small size of these DST-NLCs uncoated and coated with CSO-SA (200- 250 nm) will ensure deep penetration into the hair follicle duct [11]. The different size of nanoparticles will affect the penetration depth [13]. Particles in the size range used in this study would be predicted to penetrate the upper part of follicle of terminal hair, and would likely penetrate deeper in the vellus hair follicles, especially on the balding site, where the hair is short, thin and fine. By contrast, application of ethanol-based formulations produces documented adverse reactions. The adverse reactions resulting from ethanol-use as a carrier (e.g. scalp dryness, irritation and burning, contact dermatitis [49]), should be avoided by using nanoparticle formulations.

3.2.11 *In vitro* cytotoxicity

After 5 days of treatment with various concentrations of dutasteride (alone) and nanoparticles, there was a significant difference ($p<0.05$) in cytotoxicity values (IC_{50}). Dutasteride alone (Fig. 10A) showed cytotoxicity at very low concentrations ($IC_{50} = 10.4 \pm 1.82$ µM). Values of IC_{50} for DST-NLCs, coated and uncoated with CSO-SA (Fig. 10B) were higher; up to 59.3 ± 13.1 µM and 58.1 ± 13.0 µM, respectively. For the maximum non-toxic concentration (MNTC, EC_{90}), dutasteride without nanoparticles at 2.1 ± 0.2 µM killed 10% of normal human dermal papilla cells. Meanwhile, dutasteride in the nanoparticles either coated with CSO-SA (53.6 ± 8.3 µM) or uncoated (38.1 ± 13.1 µM) could be applied at a higher concentration compared to the dutasteride without nanoparticles. However, NLCs alone (without dutasteride) also showed cytotoxicity ($IC_{50} = 58.1 \pm 13.0$ µM) in a dose-dependent manner. The MNTC (EC_{90}) for NLCs uncoated and coated with CSO-SA was 42.3 ± 12.4 µM and 49.4 ± 6.0 µM, respectively. There was no significant difference ($p<0.05$) in MNTC between uncoated DST-NLCs and those coated with CSO-SA. This showed that when dutasteride was delivered using nanoparticles, it increased MNTC (EC_{90}) of the drug approximately 20-fold, probably due to the slow release of the drug from the nanocarrier system. It is interesting to note that, NLCs (with no dutasteride) coated and uncoated with CSO-SA also proliferated the hair follicle dermal papilla cells at 25 uM (comparable with the formulation containing dutasteride) when compared to the control. This shows that, stearic acid acts as a main component for the NLCs system and could itself promote hair growth. An efficacy study of the formulations on 5α-reductase inhibition is on-going.

4.0   CONCLUSION

The stearic acid-chitosan conjugate was successfully prepared, as confirmed by [1]NMR and FTIR analysis. DST-NLCs produced good entrapment efficiency ($97.8 \pm 0.68\%$) and drug loading ($3.49 \pm 0.10\%$), using 17.5 mg of dutasteride in the scaled-up formulation. By adding CSO-SA to DST-NLCs, the mean hydrodynamic diameter and PDI were increased, and the NLCs had a high positive charge. DST-NLCs coated with 5% CSO showed good stability after 60 days. The release profile for DST-NLCs coated

with CSO-SA indicated slow release over the first 12 h. In the permeation study, no dutasteride was detected in the receptor chamber after 48 h, indicating dutasteride has low permeability. An amount of $6.09 \pm 1.09\,\mu g/cm^2$ and $2.82 \pm 0.40\,\mu g/cm^2$ respectively, of dutasteride were found in the skin after 48 h of the permeation studies, indicating that DST-NLCs, uncoated and coated with 5% CSO-SA would be a good carrier for dutasteride. By encapsulating the dutasteride in the NLC formulations the maximum non-toxic concentration was increased approximately 20-fold. Further work using cell-uptake studies is required to establish the ability of these, or related formulations to target hair follicle dermal papilla cells for promoting the hair growth. As a conclusion, dutasteride-loaded nanostructured lipid carriers coated with stearic acid-chitosan conjugate (CSO-SA), represent a promising strategy for topical delivery of dutasteride.

Conflict of interest

The authors declare there are no conflicts of interest.

REFERENCES

[1]   M. Yassa, M. Saliou, Y. De Rycke, C. Hemery, M. Henni, J.M. Bachaud, N. Thiounn, J.M. Cosset, and P. Giraud, Male pattern baldness and the risk of prostate cancer., Ann. Oncol. 22 (2011) 1824–1827. doi:10.1093/annonc/mdq695.

[2]   V.A. Randall and N.I. Botchkareva, The Biology of Hair Growth, First Edit, William Andrew Inc., 2009. doi:10.1016/B978-0-8155-1572-2.50006-3.

[3]   N. Hibberts, A. Howell, and V. Randall, Balding hair follicle dermal papilla cells contain higher levels of androgen receptors than those from non-balding scalp., J.   Endocrinol.   156   (1998)   59–65. http://www.ncbi.nlm.nih.gov/pubmed/9496234.

[4]   E. Olsen, M. Hordinsky, D. Whiting, D. Stough, S. Hobbs, M.L. Ellis, T. Wilson, and R.S. Rittmaster, The importance of dual 5α-reductase inhibition in the treatment of male pattern hair loss: Results of a randomized placebo-controlled study of dutasteride versus finasteride, J. Am. Acad. Dermatol. 55 (2006) 1014–1023. doi:10.1016/j.jaad.2006.05.007.

[5]   D.W. Russell and J.D. Wilson, Steroid 5alpha-Reductase : Two Genes / Two Enzymes, Annu. Rev. Biochem. 63 (1994) 25–61.

[6]   H.C. Eun, O.S. Kwon, J.H. Yeon, H.S. Shin, B.Y. Kim, B.I. Ro, H.K. Cho, W.Y. Sim, B.L. Lew, W.-S. Lee, H.Y. Park, S.P. Hong, and J.H. Ji, Efficacy, safety, and tolerability of dutasteride 0.5 mg once daily in male patients with male pattern hair loss: a randomized, double-blind, placebo-controlled, phase III study., J. Am. Acad. Dermatol. 63 (2010) 252–8. doi:10.1016/j.jaad.2009.09.018.

[7]   A.K. Gupta and A. Charrette, The efficacy and safety of 5α-reductase inhibitors in androgenetic alopecia : a network meta-analysis and benefit – risk assessment of finasteride and dutasteride, J. Dermatolog. Treat. 25 (2014) 156–161. doi:10.3109/09546634.2013.813011.

[8]   S. Gur, P.J. Kadowitz, and W.J. Hellstorm, Effects of 5-alpha reductase inhibitors on erectile function, sexual desire and ejaculation, Expert Opin. Drug Saf. 12 (2013) 81–90. doi:10.1517/14740338.2013.742885.

[9]   N.H. Ansari, E. Anis, S.F.S. Firdaus, S. Wahab, and M.F.A.N. Mishra, Synthesis of Dutasteride Loaded Nanoemulsion, Int. J. Sci. Res. (2013) 85–87.

[10]   T. Madheswaran, R. Baskaran, P. Sundaramoorthy, and B.K. Yoo, Enhanced skin permeation of 5α-reductase inhibitors entrapped into surface-modified liquid

crystalline nanoparticles, Arch. Pharm. Res. 38 (2015) 534–542. doi:10.1007/s12272-014-0464-8.

[11] J. Lademann, H. Richter, A. Teichmann, N. Otberg, U. Blume-Peytavi, J. Luengo, B. Weiss, U.F. Schaefer, C.-M. Lehr, R. Wepf, and W. Sterry, Nanoparticles - An efficient carrier for drug delivery into the hair follicles., Eur. J. Pharm. Biopharm. 66 (2007) 159–64. doi:10.1016/j.ejpb.2006.10.019.

[12] U. Blume-Peytavi, L. Massoudy, A. Patzelt, J. Lademann, E. Dietz, U. Rasulev, and N. Garcia, Follicular and percutaneous penetration pathways of topically applied minoxidil foam, Eur. J. Pharm. Biopharm. 76 (2010) 450–453. doi:10.1016/j.ejpb.2010.06.010.

[13] A. Patzelt, H. Richter, F. Knorr, U. Schäfer, C. Lehr, L. Dähne, W. Sterry, and J. Lademan, Selective follicular targeting by modification of the particle sizes, J. Control. Release. 150 (2011) 45–48. doi:10.1016/j.jconrel.2010.11.015.

[14] R.H. Muller, K. Mader, A. Lippacher, and V. Jenning., Solid-liquid (semi-solid) liquid particles and method of producing highly concentrated lipid particle dispersions, PCT/EP00/04565, 2000.

[15] R.H. Müller, A. Hommoss, J. Pardeike, and C. Schmidt, Lipid nanoparticles (NLC) as novel carrier for cosmetics - Special features & state of commercialisation, SÖFW. 9 (2007) 40–46.

[16] J.S. Lucks and R.H. Müller, Medication Vehicles Made of Solid Lipid Particles (Solid Lipid Nanospheres SLN), 1991.

[17] X. Yang, H.Y. Lee, J. Kim, X. Yang, H.Y. Lee, and J. Kim, In vitro skin permeation of hinokitiol loaded in vesicles composed of behenyltrimethylammonium chloride and stearic acid, Drug Dev. Ind. Pharm. 36 (2010) 556–562. doi:10.3109/03639040903325578.

[18] K. Shimizu, R. Kondo, K. Sakai, Y. Shoyama, H. Sato, and T. Ueno, Steroid

5alpha-reductase inhibitory activity and hair regrowth effects of an extract from Boehmeria nipononivea, Biosci Biotechnol Biochem. 64 (2000) 875–877.

[19]   GlaxoSmithKline Inc., Clinical Pharmacological and Biopharmaceutics Review-Dutasteride (Code name:GI1987, North Carolina, 2001. doi:http://www.accessdata.fda.gov/drugsatfda_docs/nda/2001/21319_duagen_biopharmr_p1.pdf.

[20]   J. Pardeike, A. Hommoss, and R.H. Müller, Lipid nanoparticles (SLN, NLC) in cosmetic and pharmaceutical dermal products., Int. J. Pharm. 366 (2009) 170–84. doi:10.1016/j.ijpharm.2008.10.003.

[21]   A. Mittal, K. Schulze, T. Ebensen, S. Weissmann, S. Hansen, C. a. Guzmán, and C.-M. Lehr, Inverse micellar sugar glass (IMSG) nanoparticles for transfollicular vaccination, J. Control. Release. 206 (2015) 140–152. doi:10.1016/j.jconrel.2015.03.017.

[22]   H. Hamishehkar, S. Ghanbarzadeh, S. Sepehran, Y. Javadzadeh, Z.M. Adib, and M. Kouhsoltani, Histological assessment of follicular delivery of flutamide by solid lipid nanoparticles: potential tool for the treatment of androgenic alopecia, Drug Dev. Ind. Pharm. 9045 (2015) 1–8. doi:10.3109/03639045.2015.1062896.

[23]   B. Bhushan, Biophysics of Human Hair, Springer Berlin Heidelberg, Berlin, Heidelberg, 2010. doi:10.1007/978-3-642-15901-5.

[24]   D.M. Ridolfi, P.D. Marcato, G.Z. Justo, L. Cordi, D. Machado, and N. Durán, Chitosan-solid lipid nanoparticles as carriers for topical delivery of tretinoin., Colloids Surf. B. Biointerfaces. 93 (2012) 36–40. doi:10.1016/j.colsurfb.2011.11.051.

[25]   J.-P. Nam, S.-C. Park, T.-H. Kim, J.-Y. Jang, C. Choi, M.-K. Jang, and J.-W. Nah, Encapsulation of paclitaxel into lauric acid-O-carboxymethyl chitosan-transferrin micelles for hydrophobic drug delivery and site-specific targeted delivery., Int. J. Pharm. 457 (2013) 124–135. doi:10.1016/j.ijpharm.2013.09.021.

[26]   H. Yuan, L. Lu, Y. Du, and F. Hu, Stearic Acid-g-chitosan Polymeric Micelle for Oral Drug Delivery : In Vitro Transport and In Vivo Absorption, Mol. Pharm. 8 (2010) 225–238.

[27]   E. Curotto and F. Aros, Quantitative determination of chitosan and the percentage of free amine groups, Anal. Biochem. (1993) 240–241.

[28]   S. Uprit, R. Kumar Sahu, A. Roy, and A. Pare, Preparation and characterization of minoxidil loaded nanostructured lipid carrier gel for effective treatment of alopecia., Saudi Pharm. J. SPJ Off. Publ. Saudi Pharm. Soc. 21 (2013) 379–85. doi:10.1016/j.jsps.2012.11.005.

[29]   M.J. Gomes, S. Martins, D. Ferreira, M. a Segundo, and S. Reis, Lipid nanoparticles for topical and transdermal application for alopecia treatment: development, physicochemical characterization, and in vitro release and penetration studies., Int. J. Nanomedicine. 9 (2014) 1231–42. doi:10.2147/IJN.S45561.

[30]   D. Patel, S. Dasgupta, S. Dey, Y.R. Ramani, S. Ray, and B. Mazumder, Nanostructured Lipid Carriers (NLC)-Based Gel for the Topical Delivery of Aceclofenac: Preparation, Characterization, and In Vivo Evaluation., Sci. Pharm. 80 (2012) 749–64. doi:10.3797/scipharm.1202-12.

[31]   K. Dillen, J. Vandervoort, G. Van Den Mooter, L. Verheyden, and A. Ludwig, Factorial design, physicochemical characterisation and activity of ciprofloxacin-PLGA nanoparticles, Int. J. Pharm. 275 (2004) 171–187. doi:10.1016/j.ijpharm.2004.01.033.

[32]   Y.-T. Xie, Y.-Z. Du, H. Yuan, and F.-Q. Hu, Brain-targeting study of stearic acid-grafted chitosan micelle drug-delivery system., Int. J. Nanomedicine. 7 (2012) 3235–44. doi:10.2147/IJN.S32701.

[33]   X. Gu, W. Zhang, J. Liu, J.P. Shaw, Y. Shen, Y. Xu, H. Lu, and Z. Wu, Preparation and characterization of a lovastatin-loaded protein-free

nanostructured lipid carrier resembling high-density lipoprotein and evaluation of its targeting to foam cells., AAPS PharmSciTech. 12 (2011) 1200–8. doi:10.1208/s12249-011-9668-0.

[34]   Q. Li, Y.-Z. Du, H. Yuan, X.-G. Zhang, J. Miao, F.-D. Cui, and F.-Q. Hu, Synthesis of lamivudine stearate and antiviral activity of stearic acid-g-chitosan oligosaccharide polymeric micelles delivery system., Eur. J. Pharm. Sci. 41 (2010) 498–507. doi:10.1016/j.ejps.2010.08.004.

[35]   F.-Q. Hu, L.-N. Liu, Y.-Z. Du, and H. Yuan, Synthesis and antitumor activity of doxorubicin conjugated stearic acid-g-chitosan oligosaccharide polymeric micelles., Biomaterials. 30 (2009) 6955–63. doi:10.1016/j.biomaterials.2009.09.008.

[36]   T. Prozorov, G. Kataby, R. Prozorov, and a. Gedanken, Effect of surfactant concentration on the size of coated ferromagnetic nanoparticles, Thin Solid Films. 340 (1999) 189–193. doi:10.1016/S0040-6090(98)01400-X.

[37]   N.N. Gaber, Y. Darwis, P. Kok-Khiang, and Y. Tze Fung Tan, Characterization of polymeric micelles for pulmonary delivery of beclomethasone dipropionate, J Nanosci Nanotechnol. 6 (2006) 3095–101.

[38]   Q. Luo, J. Zhao, X. Zhang, and W. Pan, Nanostructured lipid carrier (NLC) coated with Chitosan Oligosaccharides and its potential use in ocular drug delivery system, Int. J. Pharm. 403 (2011) 185–191. doi:10.1016/j.ijpharm.2010.10.013.

[39]   R. Nair, A.C.K. Kumar, V.K. Priya, C.M. Yadav, and P.Y. Raju, Formulation and evaluation of chitosan solid lipid nanoparticles of carbamazepine., Lipids Health Dis. 11 (2012) 72. doi:10.1186/1476-511X-11-72.

[40]   P. Fonte, T. Nogueira, C. Gehm, D. Ferreira, and B. Sarmento, Chitosan-coated solid lipid nanoparticles enhance the oral absorption of insulin, Drug Deliv. Transl. Res. 1 (2011) 299–308. doi:10.1007/s13346-011-0023-5.

27

[41] Y.-C. Kuo and C.-C. Wang, Cationic solid lipid nanoparticles with cholesterol-mediated surface layer for transporting saquinavir to the brain., Biotechnol. Prog. 30 (2013) 198–206. doi:10.1002/btpr.1834.

[42] S. dos Santos, B. Edronho, T. Santos, and F.E. Antunes, Amphiphilic Molecules in Drug Delivery Systems, in: J. Coelho (Ed.), Adv. Predict. Prev. Pers. Med., Spinger, 2013: pp. 35–85. doi:10.1007/978-94-007-6010-3.

[43] I.A. Aljuffali, C.T. Sung, F.-M. Shen, C.-T. Huang, and J.-Y. Fang, Squarticles as a lipid nanocarrier for delivering diphencyprone and minoxidil to hair follicles and human dermal papilla cells., AAPS J. 16 (2014) 140–50. doi:10.1208/s12248-013-9550-y.

[44] U. Jacobi, M. Kaiser, R. Toll, S. Mangelsdorf, H. Audring, N. Otberg, W. Sterry, and J. Lademann, Porcine ear skin: an in vitro model for human skin., Skin Res. Technol. 13 (2007) 19–24. doi:10.1111/j.1600-0846.2006.00179.x.

[45] A.C. Williams and B.W. Barry, Penetration enhancers, Adv. Drug Deliv. Rev. 56 (2004) 603–618. doi:10.1016/j.addr.2003.10.025.

[46] N.M. Siqueira, R. V. Conti, K. Paese, R.C.R. Beck, A.R. Pohlmann, and S.S. Guterres, Innovative Sunscreen Formulation Based on Benzophenone-3-Loaded Chitosan-Coated Polymeric Nanocapsules, Skin Pharmacol. Physiol. 24 (2011) 166–174. doi:10.1159/000323273.

[47] A.M. De Campos, A. Sanchez, R. Gref, P. Calvo, and M.J. Alonsoa, The effect of a PEG versus a chitosan coating on the interaction of drug colloidal carriers with the ocular mucosa, Eur. J. Pharm. Sci. 20 (2003) 73–81.

[48] M. Rinaudo, Chitin and chitosan: Properties and applications, Prog. Polym. Sci. 31 (2006) 603–632. doi:10.1016/j.progpolymsci.2006.06.001.

[49] D.W. Lachenmeier, Safety evaluation of topical applications of ethanol on the skin and inside the oral cavity, J. Occup. Med. Saf. 16 (2008) 1–16.

Table 1 Design of experiment for preparing dutasteride-loaded nanostructured lipid carrier (DST-NLCs) using a 2^3 full factorial design

Formulation	Stearic acid (mg)	Lutrol® micro 68 (mg)	Phosal® 53 MCT (mg)
S1	50 (-1)	25 (-1)	25 (-1)
S2	100 (+1)	25 (-1)	25 (-1)
S3	50 (-1)	50 (+1)	25 (-1)
S4	100 (+1)	50 (+1)	25 (-1)
S5	50 (-1)	25 (-1)	50 (+1)
S6	100 (+1)	25 (-1)	50 (+1)
S7	50 (-1)	50 (+1)	50 (+1)
S8	100 (+1)	50 (+1)	50 (+1)

¥Number in bracket represents the coded value

Table 2 Analysis of variance (ANOVA) for 2^3 full factorial design on hydrodynamic diameter (at day 14)

	Sum of squares	*df*	*F*-value	*P* value
Model	99861.59	3	26.13	0.0043*
A	42748.88	1	33.56	0.0044*
B	7626.12	1	5.99	0.0707
AB	49486.58	1	38.85	0.0034*

A – Stearic acid, B – Lutrol® micro 68, C – Phosal® 53 MCT

* Significance level $p<0.05$

Table 3 Analysis of variance (ANOVA) for 2^3 factorial design on PDI (day 14)

	Sum of squares	*df**	*F*-value	*P* value
Model	0.046	5	267.18	0.0037*
A	0.018	1	527.01	0.0019*
B	1.805×10^{-4}	1	5.27	0.1486
C	0.014	1	412.03	0.0024*
AB	0.012	1	337.28	0.0030*
AC	1.861×10^{-3}	1	54.32	0.0179*

A – Stearic acid, B – Lutrol® micro 68, C – Phosal® 53 MCT

* Significance level $p < 0.05$

Table 4 Entrapment efficiency and drug loading of DST-NLCs at day 1 (n=3)

Formulation	Stearic acid (mg)	Lutrol® micro 68 (mg)	Phosal® 53 MCT (mg)	EE (%) (mean ± SD)	DL (%) (mean ± SD)
S1	50	25	25	79.6 ± 10.3	4.40 ± 0.58
S2	100	25	25	81.7 ± 20.3	3.31 ± 0.75
S3	50	50	25	63.2 ± 21.8	2.98 ± 0.61
S4	100	50	25	97.6 ± 2.4	3.27 ± 0.07
S5	50	25	50	80.0 ± 0.6	2.49 ± 0.65
S6	100	25	50	97.7 ± 1.2	3.09 ± 0.35
S7	50	50	50	64.8 ± 7.7	2.09 ± 0.32
S8	100	50	50	92.5 ± 5.6	2.66 ± 0.24

EE – entrapment efficiency, DL – drug loading

Table 5 Analysis of variance (ANOVA) for 2^3 full factorial design experiment variables' effect on entrapment efficiency

	Sum of squares	*df**	*F*-value	*P* value
Model	1116.71	3	10.46	0.0230*
A	838.45	1	23.56	0.0083*
B	54.80	1	1.53	0.2832
AB	223.66	1	6.28	0.0663

A – Stearic acid, B – Lutrol ® F68, C – Phosal® 53 MCT, *significance level $p<0.05$

Table 6 Size distribution and surface charge of uncoated DST-NLCs and coated with CSOSA or CSO

| Storage condition	DST-NLCs	DST-NLCs 5% CSO-SA	DST-NLCs 10% CSO-SA	DST-NLCs 5% CSO
Day 1 (Initial)				
Particle size (nm)	187.6 ± 7.0	220.1 ± 11.9	230.1 ± 8.2	208.4 ± 1.6
PDI	0.117 ± 0.008	0.149 ± 0.024	0.147 ± 0.026	0.167 ± 0.025
Zeta potential (mV)	-18 ± 0.9	$+26 \pm 1.1$	$+30 \pm 1.2$	$+22 \pm 2.1$
Day 30 at 4°C				
Particle size (nm)	216.8 ± 6.0	239.0 ± 24.3	241.9 ± 7.5	Aggregation
PDI	0.132 ± 0.017	0.193 ± 0.064	0.213 ± 0.006	Aggregation
Zeta potential (mV)	-17.2 ± 2.6	33.9 ± 1.8	33.8 ± 1.8	Aggregation
Day 30 at 25°C				
Particle size (nm)	435.3 ± 32.0	443.6 ± 62.9	Aggregation	Aggregation
PDI	0.208 ± 0.036	0.233 ± 0.032	Aggregation	Aggregation
Zeta potential (mV)	-17.0 ± 0.7	24.0 ± 1.0	Aggregation	Aggregation
Day 60 at 4°C				
Particle size (nm)	228.5 ± 6.8	$243.8.0 \pm 18.8$	259.8 ± 4.2	Aggregation
PDI	0.128 ± 0.004	0.155 ± 0.025	0.215 ± 0.020	Aggregation
Zeta potential (mV)	-17.2 ± 2.6	32.2 ± 10.4	29.4 ± 5.6	Aggregation
Day 60 at 25°C				
Particle size (nm)	435.3 ± 32.0	578.2 ± 27.0	Aggregation	Aggregation
PDI	0.208 ± 0.036	0.274 ± 0.113	Aggregation	Aggregation
Zeta potential (mV)	-18.9 ± 1.6	20.0 ± 1.6	Aggregation	Aggregation
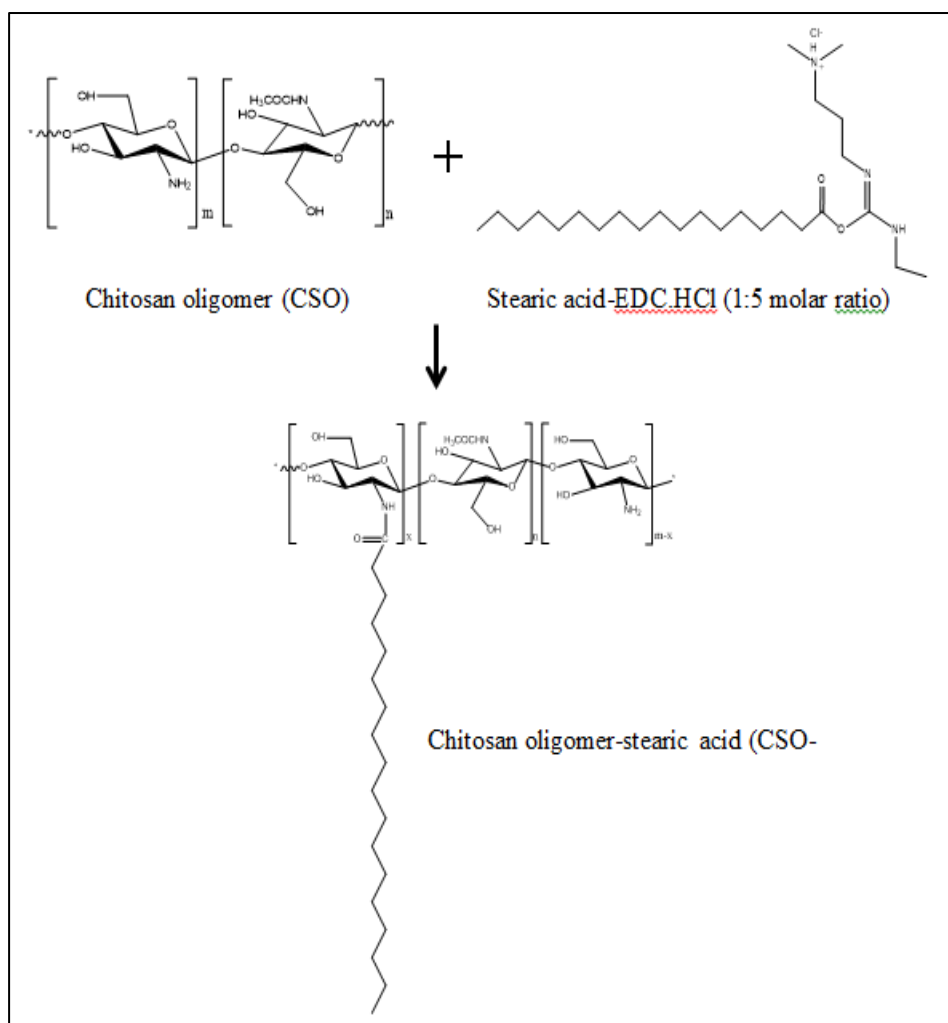
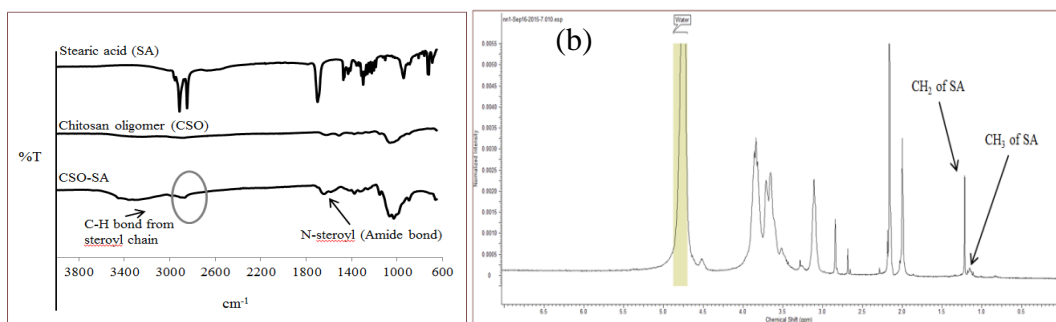**Fig. 1 Conjugation of chitosan oligomer with stearic acid.**

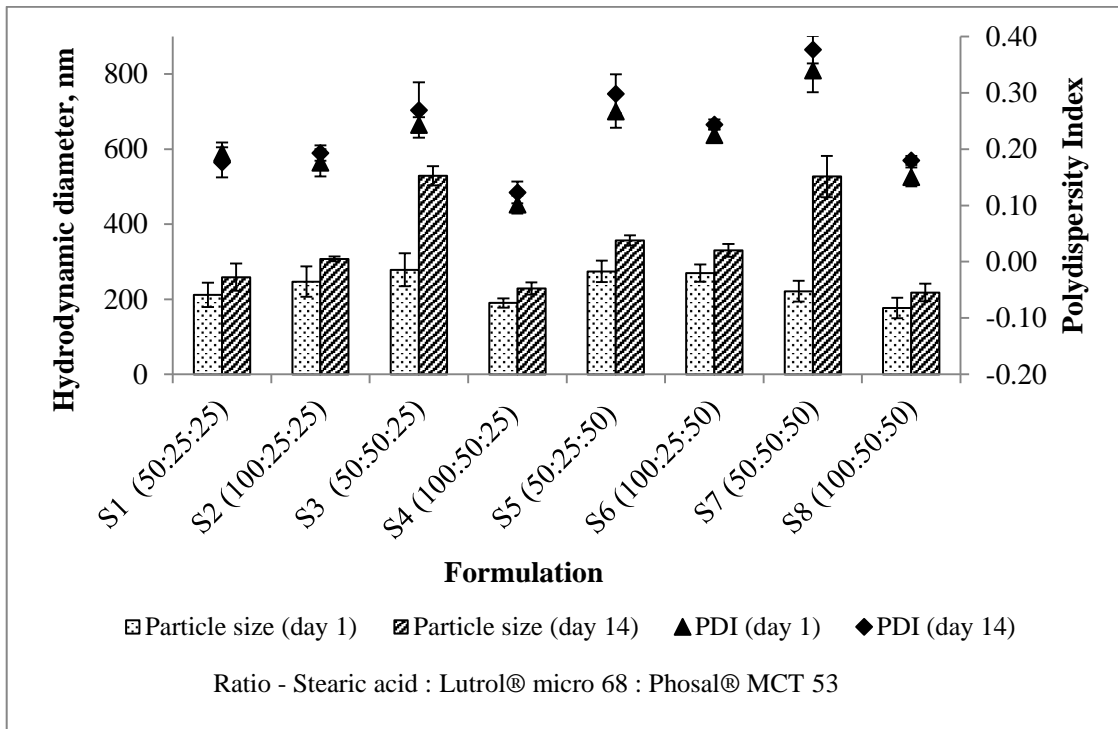**Fig. 2 FTIR (a) and ^{1}H NMR (b) spectra of CSO-SA.**

Fig. 3 Hydrodynamic diameter (nm) and particle size distribution for formulations of DST-NLCs (day 1 and day 14, n=3 ± s.d.).
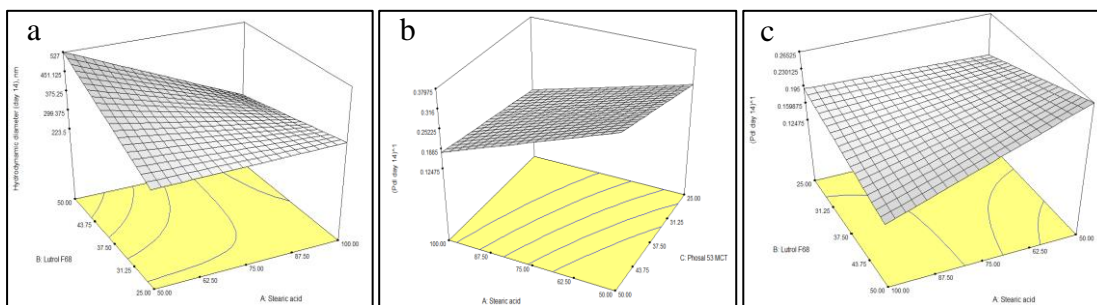
Fig. 4 3D-surface graph of interaction on hydrodynamic diameter (a) and polydispersity index (b and c) at day 14.
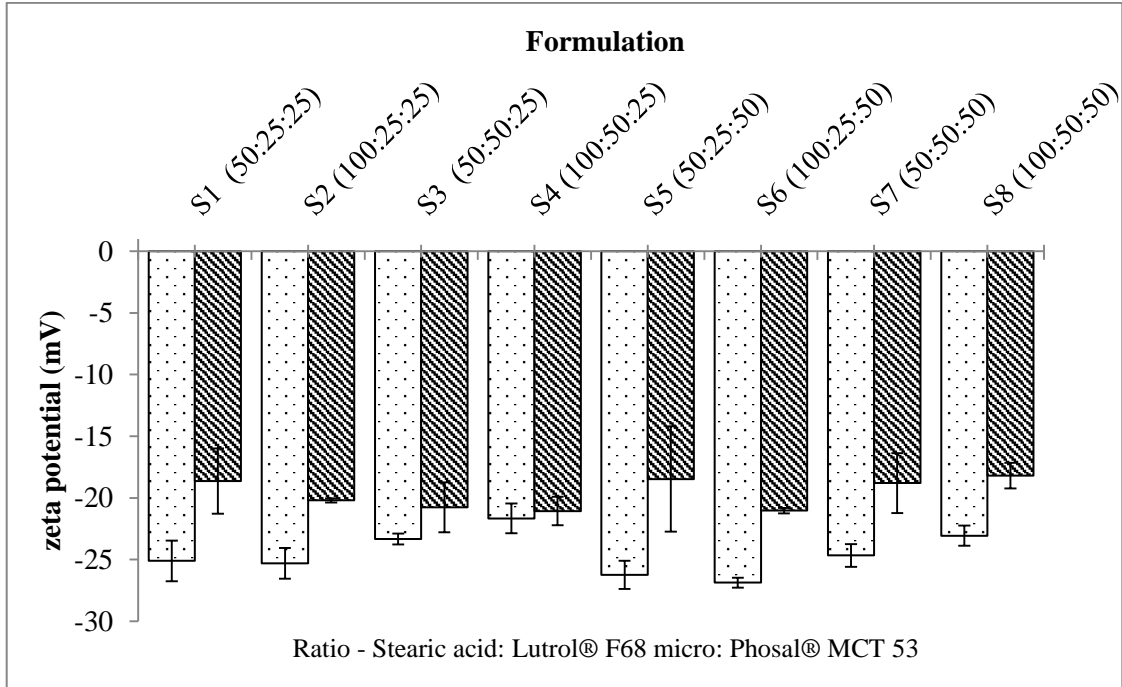
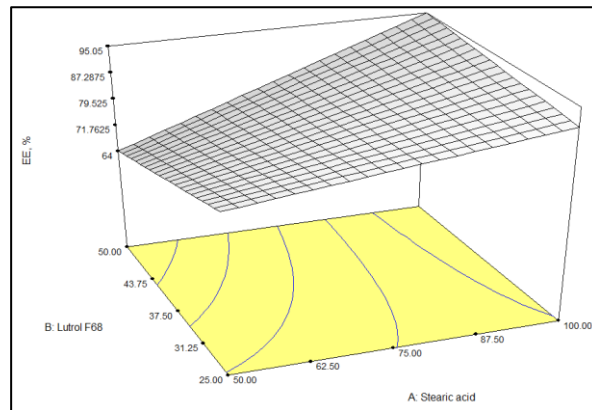**Fig. 5 Zeta potential of formulations of DST-NLCs at day 1 and day 14 (n=3 ± s.d.).**

Fig. 6 3D-surface graph of interaction between stearic acid (*A*) and Lutrol® micro 68 (*B*) on entrapment efficiency.
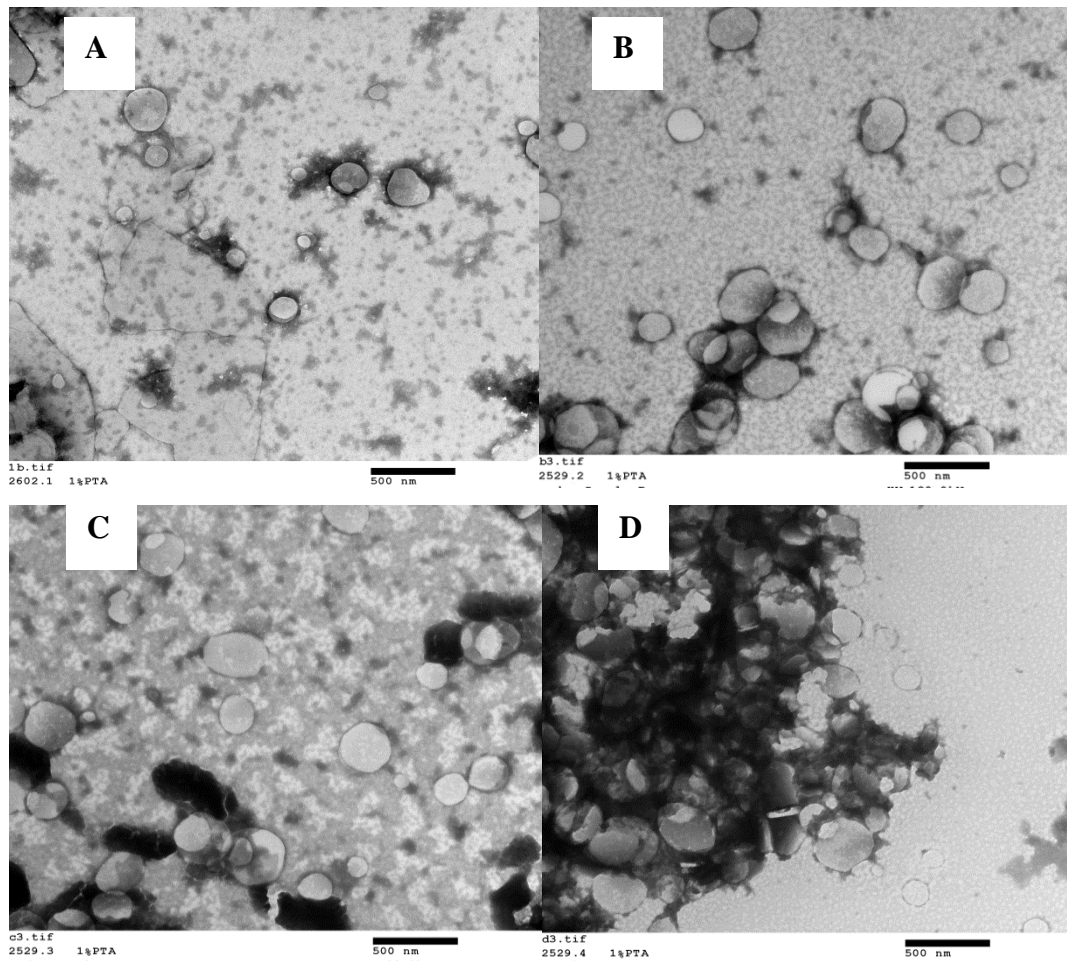
Fig. 7 TEM Morphology of DST-NLCs, uncoated (A), coated with; 5% CSO (B), 5% CSO-SA (C) and 10% CSO-SA (D).
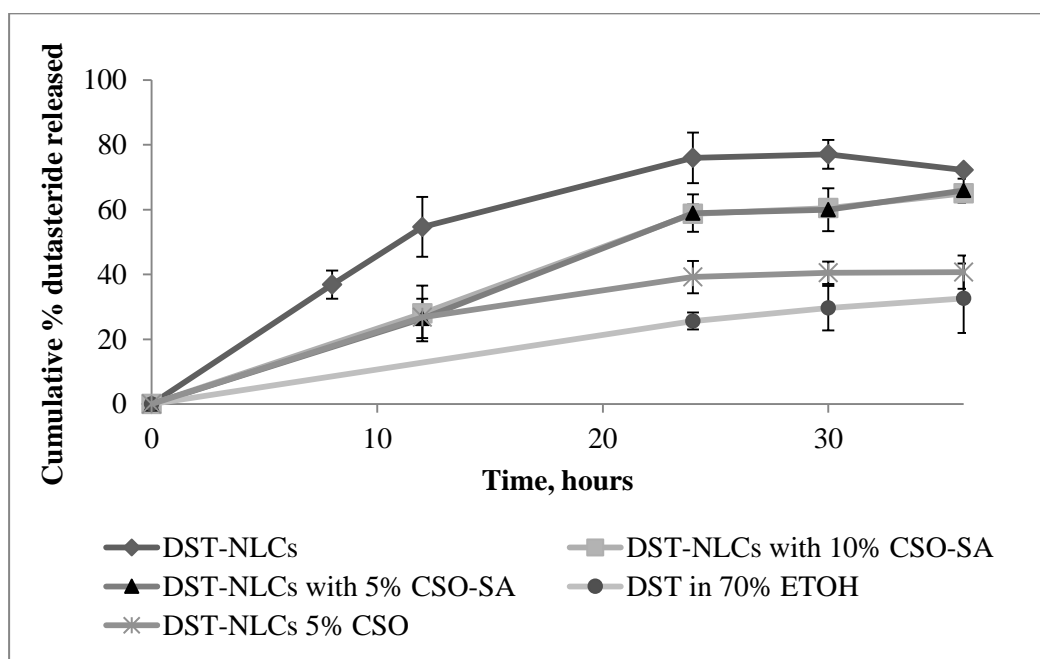
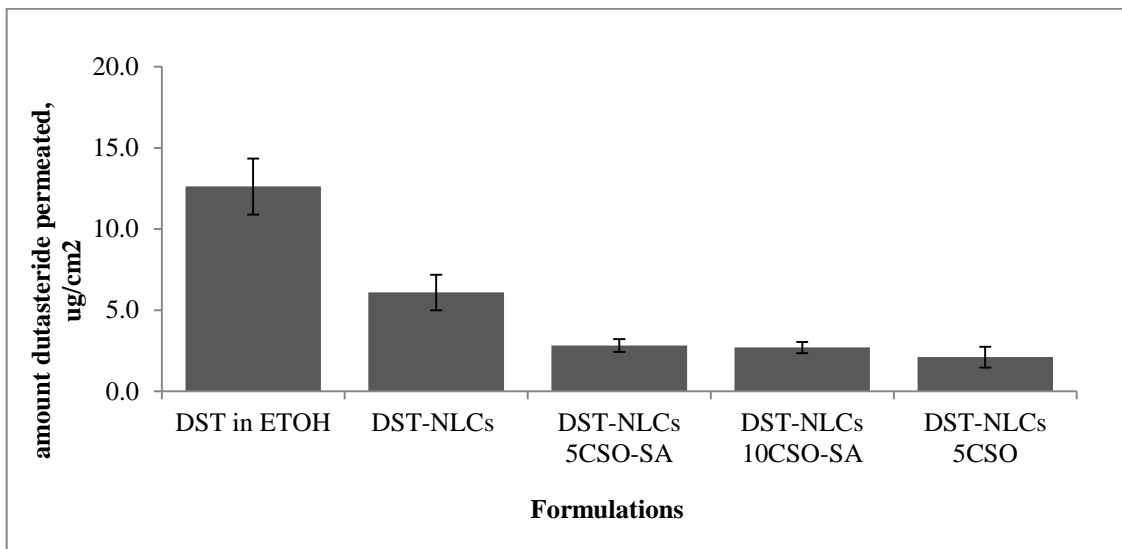**Fig. 8 Drug release from different DST-NLCs formulations and control (dutasteride in ethanol) (n=3 ± s.d.).**

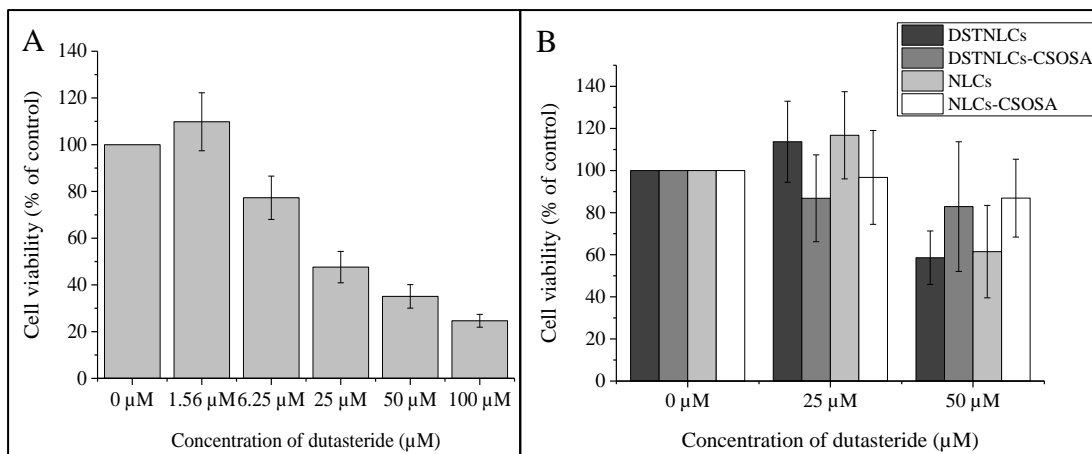**Fig. 9 Amount of dutasteride permeated in the skin after 48 hours (n=4 ± s.d.).**

Fig. 10 Cytotoxicity of dutasteride alone (A), DST-NLCs uncoated and coated with CSO-SA and empty NLCs/NLCs-CSOSA (B) on hair follicle dermal papilla cells (n=4 ± s.d.).